Journal of Materials Chemistry A

Accepted Manuscript

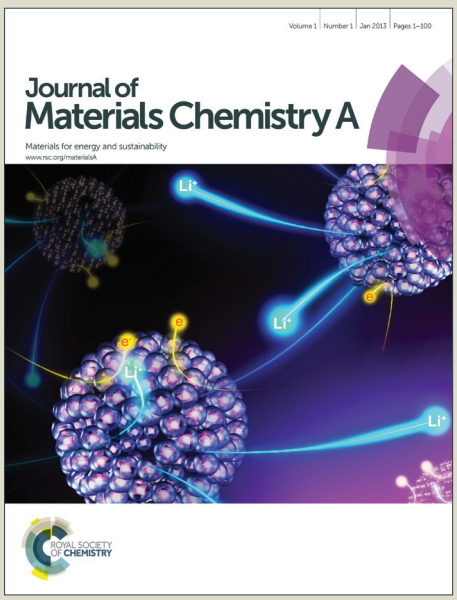

ROYAL SOCIETY OF CHEMISTRY

www.rsc.org/materialsA

Highly efficient coordination of Hg^{2+} and Pb^{2+} metals in water with squaramide-coated Fe_3O_4 nanoparticles.

Kenia A. López,[‡] M. Nieves Piña, [‡] David Quiñonero, [‡] Pablo Ballester,[†] Jeroni Morey*,[‡]

[‡] Department of Chemistry, University of the Balearic Islands, Cra. de Valldemossa Km. 7.5, 07122 Palma de Mallorca, Balearic Islands, Spain

[†] Institute of Chemical Research of Catalonia (ICIQ), Avgda. Països Catalans 16, 43007 Tarragona, Spain

The synthesis and binding properties of squaramide-coated F_3O_4 nanoparticles to coordinate heavy metals in water are described. The nanoparticles feature selective binding towards Hg^{2+} and Pb^{2+}cations in the presence of other interfering heavy metals. The binding affinity of the nanoparticles is especially large for mercury and lead cations. The mode of action of the squaramide-coated nanoparticles differs significantly from that of previously reported nanoparticles used as Hg^{2+} scavengers. The selective Hg^{2+}sequestering capabilities displayed by the squaramide-coated nanoparticles are related to the formation of organomercury compounds. The solid state structure of the orgamomercury complex obtained by treatment of a di-squaramide with Hg^{2+} salts is described, demonstrating the mercuriation of the aryl moiety of dopamine.

Introduction

The encapsulation and elimination from the environment of toxic heavy and transition metal ions, such as: Hg^{2+}, Pb^{2+}, Cd^{2+}, Cr^{3+}, Cu^{2+}, Zn^{2+}, Co^{2+}, and their derivatives is of great current interest owing to their high toxicity.[1,2] For example, Pb^{2+} ions can affect almost every organ and system of the human body, particularly in children, causing a varied quantity of symptoms such as anaemia, kidney damage, blood disorder, memory loss, muscle paralysis, and mental retardation.[3,4] In the same line, the Hg^{2+} ion is also considered highly dangerous because of its high toxicity[5] and wide variety of damage that it provokes to kidneys and the digestive and the neurological systems. Both elemental and ionic mercury can be converted into methyl mercury by different bacteria present in the environment. This induces subsequently bio-accumulation of mercury through the food chain.[6,7]

Recently, considerable efforts have been undertaken to develop novel absorbents with improved adsorption rate, capacity, and selectivity for the removal of toxic heavy metals from aqueous solution. Polymeric[8,9] and dendritic core shell architectures,[10,11] mesoporous silicas,[12] zeolites,[13] biomass,[14] and biopolymers[15] have been employed for the detoxification processes.

Different iron oxide based nanoparticles have also been used for the removal of heavy metals from solution.[16-23] The unique properties exhibited by these materials makes them excellent candidates for the development of new sensors and absorbents for toxic heavy metals. Thus, several research groups have combined the coordinating ability of surface bound molecules in Fe_3O_4 nanoparticles with their magnetic properties for the binding and removal of metals from aqueous solutions.[24-27] The adequate functionalization of the nanoparticles allows the improvement of the affinity for metal coordination and selectivity.

To the best of our knowledge, the ability of squaramides for the complexation of heavy metals has not been reported. In the literature, we found a few examples of squaraines (squaric acid derivatives) able to coordinate toxic ions such as Hg^{2+} and Pb^{2+}.[28-32] In most cases, however, the squaraine group is not directly involved in the coordination of the metal but they simply act as signalling units. We decided to undertake the work reported here, owing to the lack of examples involving the use of squaramides as binding units for heavy metals, and their use in the coating of nanoparticles.

Results and discussion

Herein, we report the preparation of three squaramide-coated nanoparticles NP-SQ (1-3). We also disclose their properties for the binding and potential removal of metal ions, especially Hg^{2+} and Pb^{2+} from aqueous solutions (Figure 1). The nanomaterials NP-SQ(1-3) were prepared by simple condensation of Fe_3O_4 nanoparticles with squaramide-derivatives containing one dopamine units.[33,34] In turn, the squaramide-dopamine components were obtained in a one-step procedure according to previously reported methods.[35,36] The synthesis of the squaramide-hybrid nanomaterials involve the initial dispersion of the Fe_3O_4 nanoparticles in ethanol (40 mL) by sonication for 30 min. At that point, the squaramide-dopamine derivatives SQ1, SQ2 or SQ3, previously dissolved in ethanol, were added and the resulting mixtures were stirred under argon atmosphere for 12 h. Finally, the coated NP-SQ (1-3) were separated using a magnet, washed with ethanol two times and re-dispersed in ethanol by sonication.

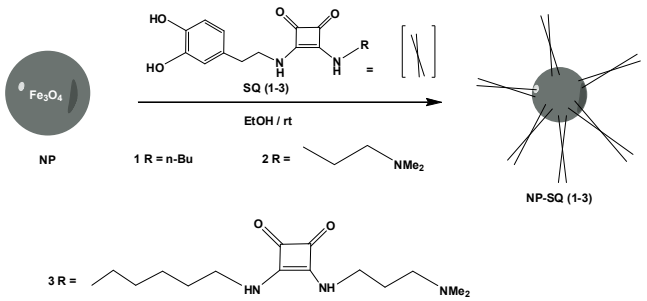

Figure 1. Synthetic procedure to obtain squaramide-coated NP-SQ (1-3).

The structure of these unprecedented hybrid nanocompounds was established using FTIR spectroscopy. Two typical C=O stretching bands centered around 1800 cm^{-1} and 1650 cm^{-1} were attributed to the squaramide unit. In addition, a strong band with maximum at 1580 $cm^{-1}$was observed and assigned to the amide N-H bending of squaramides that coat the nanoparticles' surfaces. The IR spectra also showed bands at 589 cm^{-1} and 420 cm^{-1} which are typical absorptions of Fe-O bonds.[37] The transmission electron microscopy (TEM) image of NP-SQ (1-3), revealed a spherical structure for the nanoparticles with a narrow size distribution of ca. 8 nm (Figure 2). The number of dopamine-squaramide residues installed in the surface of each nanoparticle was estimated using inductively coupled plasma (ICP) and elemental analysis to be ca. 550.[38]

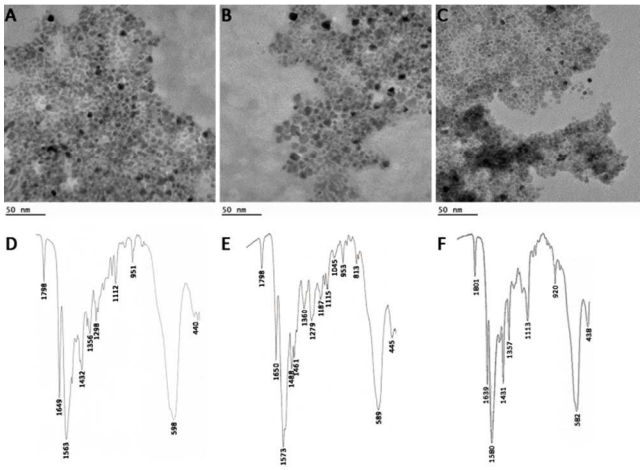

Figure 2. TEM images and IR spectra of NP-SQ1 (A, D), NP-SQ2 (B, E) and NP-SQ3 (C, F).

The binding/absorption abilities of the hybrid nanomaterials were initially tested using experiments directed to the removal of mercury ions from aqueous solutions.[38] All the experiments of mercury removal were carried out with solutions of Milli-Q water having an initial concentration of $[Hg(ClO_4)_2]_0 = 2.5 \times 10^{-5}$ M corresponding to $[Hg^{2+}]_0 = 5$ ppm. The functionalized NP-SQ (1-3) (5 mg) were suspended in the above aqueous solution (10 mL) by sonication (1 min). The final pH of the different mixtures was adjusted at 3.1, 5.5 and 6.9 by adding NaOH 1M. Next, the obtained suspensions were stirred at r. t. for 30 min. After magnetic filtration of the NPs and subsequent filtration of the supernatant through a Teflon filter, an aliquot (2 mL) was taken for analysis of the Hg^{2+} concentration using flow-injection-hydride generation.[39] Figure 3 shows the obtained results as the percentage of eliminated Hg^{2+} *vs* initial $[Hg^{2+}]_0$, for each NP and at the three different employed pH. Taken together, the obtained data indicate that the three NPs are highly efficient in Hg^{2+} removal independently of the pH of the solution. At the studied three different pH values, the most effective nanomaterial was NP-SQ1. NP-SQ1 features an n-butyl substituted squaramide anchored on the surface. For this reason its capabilities directed at the removal of mercury cations were expected to be less pH sensitive than those of the other nanomaterials NP-SQ (2-3). These latter two nanomaterials include a dimethylalkylammonium group as substituent of the squaramide unit. The tertiary amine residue was expected to be protonated to different extent in response to the pH of the solution. The introduction of a positive charge in the squaramide component may reduce its binding capabilities towards the metal cations owing to repulsive electrostatic interactions. In fact, the extraction capabilities of NP-SQ (2-3) are somewhat reduced at pH 3.1 compared to the results obtained at less acidic pHs. Given the superior capabilities of NP-SQ1for the elimination of Hg^{2+}, we decided to center our investigations in this nanomaterial.

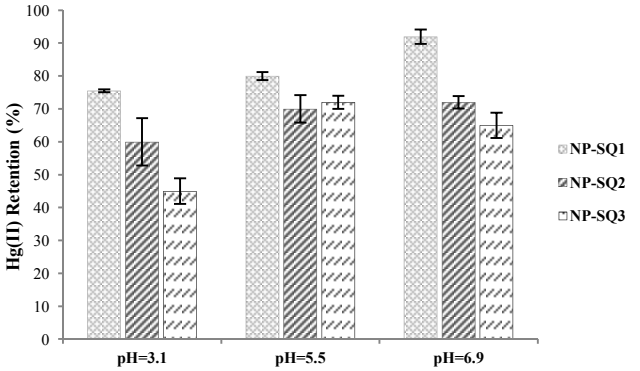

Figure 3. Percentage of elimination of Hg^{2+} ions from 10 mL of a water solution with $[Hg^{2+}]_0 = 5$ ppm using 5 mg of NP-SQ (1-3) and at three different pH values.

The elimination abilities of NP-SQ1 towards other heavy metal ions were evaluated in separate experiments that were performed using water solutions having an initial concentration of 5 ppm under similar conditions described above for Hg^{2+}, but without modifying the original pH of the solutions. The final concentration of the heavy metals, Cd^{2+}, Co^{2+}, Cr^{3+}, Cu^{2+}, Hg^{2+}, $Pb^{2+}$and Zn^{2+}, remaining in the filtered solutions free of NPs were determined using ICP-AES analysis. As control experiments we also evaluated the removal capabilities of non-functionalized Fe_3O_4 nanoparticles. The obtained results are depicted in Figure 4.

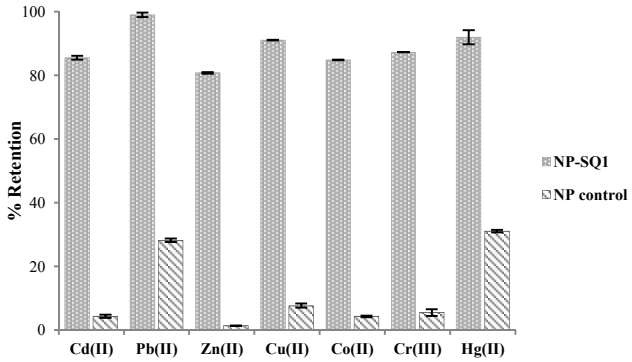

Figure 4. Percentages of retention of a series of heavy metal ions by NP-SQ1 from water solutions.

Table 1. Calculated values for the distribution coefficients (K_d in mL/g) of NP-SQ1 and NP control with the metal series used in this work.

Metal	Cd^{2+}	Pb^{2+}	Zn^{2+}	Cu^{2+}	Co^{2+}	Cr^{3+}	Hg^{2+}
K_d (NP-SQ1)	$1.17x10^4$	$1.28x10^5$	$8.46x10^3$	$8.46x10^3$	$1.11x10^4$	$1.36x10^4$	$1.86x10^5$
K_d (NP control)	8.41	$7.88x10^2$	28.45	87.31	87.31	$1.15\ x10^2$	$1.69\ x10^3$

The percentages of retention of the functionalized NP-SQ1for the different assayed heavy metals in separate experiments are very high 80-100%. Moreover, the low magnitudes determined for the percentages of retention with the control NP indicate that the ability of the NP-SQ1 to trap heavy metal cations must be related to the squaramide substituents decorating their surface. The absorption/adsorption capabilities of the NP-SQ1 for the heavy metals reside in the synergetic properties of the unfunctionalized iron oxide nanoparticles with those of the appended dopamine-squaramide unit.

In addition to the determination of the percentages of elimination for the series of heavy metals, we also calculated the corresponding distribution coefficient values (K_d). While the values of percentage of retention reflect the amount of analyte removed from the solution, the magnitude of K_d quantifies the affinities displayed by the adsorbent towards the analytes under assay conditions. The value of K_d (Equation 1) represents the weighted partition coefficient of the analyte between the liquid (supernatant) and the solid phase (adsorbent), where C_o is the initial concentration of the analyte, C_f is the concentration of the analyte remaining in solution after extraction with the nanoparticles, V is the volume of solution used for the extraction experiment in mL and M the mass of nanoparticles used in the experiments in g.[40] K_d values above 10^3mL/g are considered to be very good and those that exceed 10^4mL/g are considered as outstanding.[40]

$$K_d = \frac{C_o - C_f}{C_f} \times \frac{V}{M} \qquad Eq.1$$

The calculated K_d values for NP-SQ1 and the control NP lacking the squaramide residues are summarized in Table 1. The magnitudes obtained for the distribution coefficient values of functionalized NP-SQ1 for the different series of metals demonstrated the superior property of this material for the retention of metals, especially for Hg^{2+} and Pb^{2+}. In these two latter cases, the K_d values are larger than 10^5mL/g (Table 1). For all metals, except Cd^{2+} and Zn^{2+}, the K_d values of NP-SQ1 are 100-160 fold larger than those of NP control. For $Zn^{2+}$and Cd^{2+} the ratios are 300 and 1400, respectively. Taken together, these data suggest that for most of the metals the increase of the affinity provided by the squaramide units bound to the surface of the NP-SQ1 is quite constant and that the superior properties of this material for the retention of $Hg^{2+}$and Pb^{2+}should be mainly ascribed to the preferential absorption of these two metals by the nanoparticle core.

Other materials, recently described in the literature, were also able to remove Hg^{2+} and $Pb^{2+}$from water solutions showing comparable percentages of retention to those described for NP-SQ1. Among the reported examples, it is worth noting the Fe_3O_4 nanoparticles doped with Mn described by Addelman.[25] The Fe_3O_4 based nanoparticles coated with a polymer of thiophene described by Jang[26] showed lower percentage retention values for Hg^{2+} and Pb^{2+} than NP-SQ1, while those functionalized with humic acid described by Jiang[27] were superior.

In order to evaluate the extraction selectivity of NP-SQ1 towards mercury and lead in the presence of interfering analyses, we performed a competitive extraction experiment using 5 mg of NP-SQ1 and 10 mL of a water solution containing 5 ppm of each metal ion. The percentages of retention achieved for each metal are graphically depicted in Figure 5. The obtained results demonstrated the high selective retention of Hg^{2+} and Pb^{2+} ions by NP-SQ1. Approximately 90% of the amount of these metals present in the initial solution was retained in the nanoparticles. Conversely, Cd^{2+}, Zn^{2+}, Cu^{2+}, Co^{2+} and Cr^{3+} ions were poorly retained. Their percentages of retention for the competitive experiment were below 1.6%. Taken together, these results indicate that the mass of NP-SQ1 (5 mg) used is adequate to achieve the almost quantitative extraction of the Hg^{2+} and Pb^{2+} ions from the solution without significantly modifying the concentrations of the other competing metals. This finding is in complete agreement with the order of K_d values determined in separate extraction experiments performed with the metal series (see above). On the one hand, Hg^{2+} and Pb^{2+}, having K_d values that are at least one order of magnitude larger than those of the other metals, are preferentially extracted in the presence of the interfering metals. On the other hand, the fact, that the other metals are hardly retained, suggested that the extraction of Hg^{2+} and Pb^{2+} consumed most of the metal sites available in NP-SQ1.

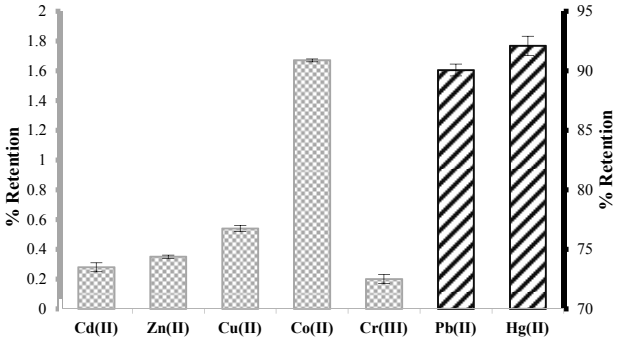

Figure 5. Retention of each heavy metal ion by NP-SQ1 in the presence of all metal ions.

The high selectivity observed for NP-SQ1 towards the Hg^{2+} and Pb^{2+}ions can be attributed to their soft acid nature and bigger size. Theoretical calculations[41] provided a distance of 3.3 Å between the two carbonyl oxygens in the squarate unit. The ionic diameter for the metal cations Hg^{2+} (2.2 Å) and Pb^{2+} (2.4 Å) makes them suitable[42] matches to be incorporated between the two oxygen atoms of the squarate unit. This ditopic binding geometry is not appropriate for Cd^{2+}, Zn^{2+}, Cu^{2+}, Co^{2+} and Cr^{3+} ions. These latter metals have smaller sizes leading to the complexation with the squarate unit just through one of the two oxygen atoms of the carbonyl groups. In order to study in detail the coordination properties of squaramides

with Hg^{2+} and Pb^{2+} metal ions, we synthesized squaramide SQ4 (Figure 6A) as a model system of the squaramide unit decorating the surface of NP-SQ1. We investigated the interaction of SQ4 with the metal ions using high resolution NMR and MS-ESI spectroscopies.

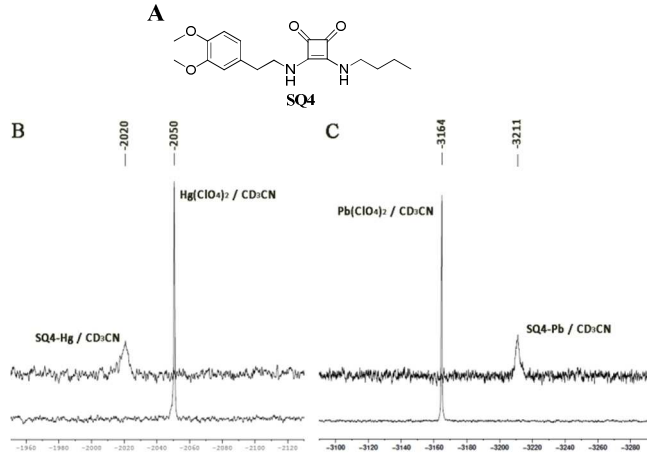

Figure 6. A) Structure of SQ4. B) ^{199}Hg-NMR of $Hg(ClO_4)_2$ and SQ4-Hg complex in CD_3CN. C) ^{207}Pb-NMR of $Pb(ClO_4)_2$ and SQ4-Pb complex in CD_3CN.

Using ^{199}Hg and ^{207}Pb-NMR experiments we obtained evidence of complex formation between SQ4 and the metal ions. Thus, the addition of an excess of SQ4 to a 1 mM solution of $Hg(ClO_4)_2$ in CD_3CN induced the observation of a single signal for the mercury ion that was downfield shifted (δ = -2020 ppm) compared to that for the same ion in $Hg(ClO_4)_2$salt free in solution (δ = -2050 ppm).Conversely, a similar experiment performed with $Pb(ClO_4)_2$ and SQ4 provoked a comparable highfield shift of the mercury ion signal in the ^{207}Pb-NMR spectrum (δ = -3211 ppm) compared to that of the free salt (δ = -3165) (Figure 6). From these experiments it was not possible to assign the complex stoichiometry but it can be stated that the chemical exchange between the free and the bound metal ion is fast on the chemical shift timescale of the NMR experiments.

The formation of complexes between the two metal ions (Hg^{2+} and Pb^{2+}) and SQ4 was also detected in solution using mass spectroscopy with ESI ionization and positive-ion detection. By spraying a MeCN solution of SQ4 and the Pb^{2+}salt we detected mono-charged positive ion-peaks corresponding to stoichiometries of1:1 complex $[Pb{\cdot}SQ4\text{-}H]^+$ and 1:2 complex $[Pb{\cdot}(SQ4)_2(ClO_4)]^+$. (Figure 7)

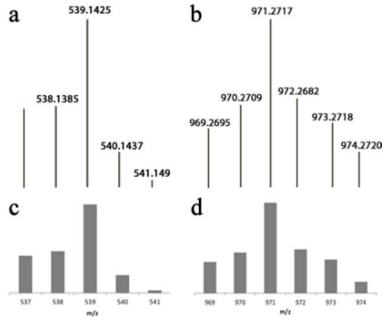

Figure 7. HRMS-ESI(+) of a CH_3CN solution of SQ4 in the presence of Pb^{2+}. The signals at m/z (a) 539.1425 and (b) 971.2717 correspond, respectively, to $[Pb{\cdot}SQ4\text{-}H]^+$ and $[Pb{\cdot}(SQ4)_2(ClO_4)]^+$. Calculated isotopic distributions for (c) $[Pb{\cdot}SQ4\text{-}H]^+$ and (d) $[Pb{\cdot}(SQ4)_2(ClO_4)]^+$ are shown.

In the case of Hg^{2+}, we observed ion-peaks that could be assigned to 1:1 stoichiometry $[Hg{\cdot}SQ4\text{-}H]^+$, the 1:2 stoichiometry $[Hg{\cdot}(SQ4)_2\text{-}H]^+$ and the 2:2 stoichiometry $[Hg_2{\cdot}(SQ4)_2\text{-}3H]^+$. The nice correlation observed between measured and calculated isotopic patterns for the ion-peaks strongly supports the assigned molecular compositions (Figure 8).

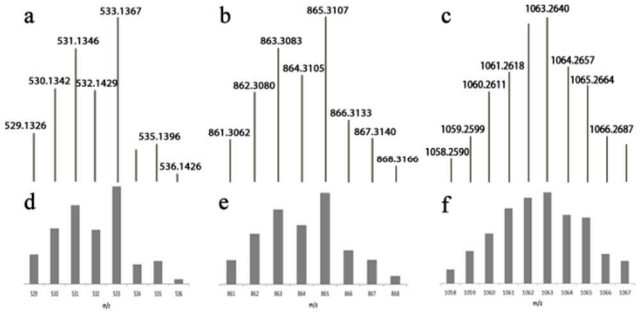

Figure 8. HRMS-ESI(+) of a CH_3CN solution of SQ4 in the presence of Hg^{2+}. The signals at m/z (a) 533.1367, (b) 865.3107 and (c) 1063.2640 correspond, respectively, to $[Hg{\cdot}SQ4\text{-}H]^+$, $[Hg{\cdot}(SQ4)_2\text{-}H]^+$ and $[Hg_2{\cdot}(SQ4)_2\text{-}3H]^+$. Calculated isotopic distributions for (d) $[Hg{\cdot}SQ4\text{-}H]^+$, (e) $[Hg{\cdot}(SQ4)_2\text{-}H]^+$ and (f) $[Hg_2{\cdot}(SQ4)_2\text{-}3H]^+$ are shown.

We also performed ^{1}H-NMR titration experiments of SQ4 with Pb^{2+} and Hg^{2+} metal ions. The incremental addition of an acetonitrile solution of $Pb(ClO_4)_2$ to a 0.5 mM solution of SQ4 in the same solvent induced significant chemical shift changes on some of the proton signals of the squaramide. For example, the signal of the NH protons moved downfield from 5.8 ppm in the free receptor to 7.2 ppm in the presence of 10 equivalents of Pb^{2+}. The aromatic and the methoxy protons also experienced significant changes. The observed chemical shift changes were analysed using a 2:1 binding model. The fit of the experimental data to the theoretical binding isotherm was good and provided the binding constant values for the 1:1 and 2.1 complex as $K_{1:1} = 3.16\times10^3$ M^{-1} and $K_{2:1} = 6.31 \times 10^5$ M^{-2}, respectively. From these values, a cooperativity factor α = 0.25 was determined for the formation of the 2:1 complex indicating that the interaction with the second squaramide unit is less favoured than the first one. Most likely, the formation of the 1:1 complex reduces the available charge density on the metal and weakens the energy of interaction with the second ligand. The metal-ligand binding energy is mainly based on purely electrostatic cation-dipole interactions.[38]

A similar titration experiment performed with the $Hg(ClO_4)_2$ salt afforded very different results. The addition of the Hg^{2+} induced the appearance of a new set of proton signals that were assigned to the bound SQ4 unit. The new signals were easily spotted in the aromatic and the methoxy regions of the ^{1}H-NMR spectrum of the mixture and they grew with the incremental addition of Hg^{2+} at the expense of the proton signals of free SQ4. This result indicates either that the chemical exchange between the free and the new signals of the receptor is occurring at a rate that is slow on the NMR chemical shift scale or that a chemical reaction is taking place between SQ4 and Hg^{2+}.

Single crystals suitable for X-ray diffraction analysis grew from an equimolar solution of SQ4 and $Hg(ClO_4)_2$ in $CHCl_3$-DMSO mixture (Figure 9). The solution of the diffracted data

revealed the formation of a supramolecular complex containing two mercury ions and two SQ4 molecules. The most significant feature of this aggregate is the existence of covalent bonds between the mercury atoms and the aromatic carbon alpha to the alkyl chain, which connects it to the squaramide unit of SQ4. The mercury atoms involved in covalent bond with the carbon atoms are also coordinated with one of the oxygen atoms of the carbonyl groups of the squaramide moiety in the same organomercury compound. The typical square-planar coordination geometry of Hg^{2+} is satisfied, in the solid state, by two oxygen atoms of carbonyl groups pertaining to an adjacent and confronted organomercury compound producing the complex with a formal 2:2 stoichiometry. The two positive charges of the aggregate are neutralized by two perchlorate anions, which are involved in anion-π interactions with the squaramide rings. Finally, the NH protons are hydrogen bonded to DMSO molecules (not shown) present in the structure of the lattice.[38]

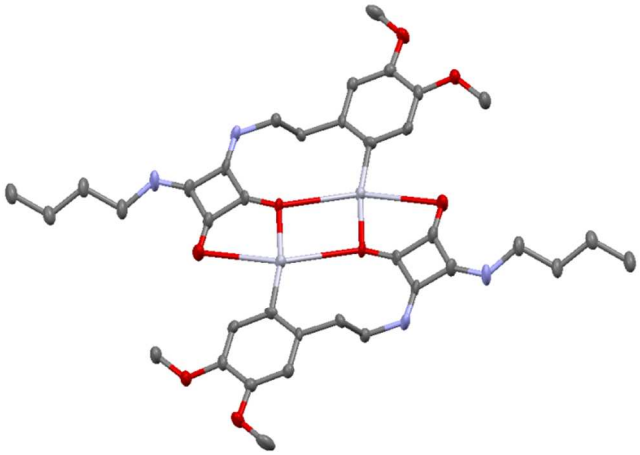

Figure 9. X-ray crystal structure of $[(Hg{\cdot}SQ4{\cdot}ClO_4)_2DMSO]$.

The direct mercuriation of the 1,2-dimethoxybenzene ring, is a typical[43,44] electrophilic aromatic substitution reaction that is facilitated by highly ionic mercury salts and by the existence of electron donating groups in the aromatic ring. In fact, both arylmercurials and polymercuriated aromatics containing a large variety of organic functional groups have been prepared using this methodology.[43,44] We carried out a theoretical study (BP86/def2-QZVP) to rationalize the observed regioselectivity in the mercuriation reaction of SQ4. In this respect, we computed the electrostatic potential at the nuclei (EPN) since a previous study[45] demonstrated that EPN values can be used to reflect quantitatively regiospecific effects of the substituents in aromatic rings. Our theoretical calculations indicated that the largest negative EPN value (maximum of negative density) is located at the carbon atom 5 (Figure 10). This result suggests that, in agreement with the crystal structure, this is the preferred position for the mercuriation to take place.

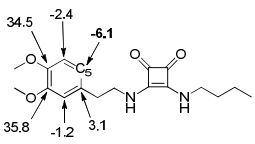

Figure 10. Electrostatic potentials (in kcal mol-1) at selected nuclei for SQ4.

The strong affinity measured for NP-SQ1 with Hg^{2+} and Pb^{2+} metal ions results from a combination of absorption and complexation processes. The complexation process is considered to occur through the initial coordination of the metal ions with both carbonyl groups of the squaramide moiety. In the specific case of Hg^{2+}, this initial coordination is followed by the mercuriation of the adjacent electron-rich aromatic ring. Alternatively, in the absorption process the metals ions reside on the surface of the iron nanoparticle or embedded in their lipophilic covers. NP-SQ1 constitutes the first example of efficient materials based on squaramide units capable of removing lead and mercury from aqueous solution.

Conclusions

In summary, we have developed a highly efficient scavenging material NP-SQ1 for the effective removal of heavy metals, specifically Hg^{2+} and Pb^{2+} in the presence of Cd^{2+}, Zn^{2+}, Cu^{2+}, Co^{2+} and Cr^{3+}, from water solutions. NP-SQ1 is based on Fe_3O_4 nanoparticles coated with squaramide units. We evidenced the formation of arylmercury bonds in the interaction of SQ4, an analogue of the squaramide units in NP-SQ1, with Hg^{2+} ions in polar organic solvents.

Experimental

1. Materials and instruments

Reactions were carried out in oven-dried glassware under atmosphere of argon, unless otherwise indicated. All commercially available reagents: Oleylamine, Oleic Acid, 1,2-hexadecanediol, Dibenzylether, Dopamine hydrochloride, Iodomethane, were supplied by Sigma Aldrich. All the solvents were purchased from Scharlau. Ferric acetylacetonate was supplied by Fluka. All the Sodium Salts: carbonate, dithionite were purchased from Panreac.

^1H and ^{13}C NMR spectra were recorded on a Bruker Avance Spectrometer at 300 and 75 MHz at 23°C. Chemical shifts are reported as a part per million (δ ppm) referenced to the residual protium signal of deuterated solvents. Spectral features are tabulated in the following order: chemical shift (∂, ppm); multiplicity (s-singlet, d-doublet, t-triplet, m-multiplet); number of protons. Electrospray mass spectra (HRMS-ESI) were recorded with a Micromass, Autospec3000 spectrometer provided with an electrospray module. Infrared (IR) were obtained on a Bruker Tensor 27 instrument, in solid state. Inductively Coupled Plasma Optical Emission Spectrometry (ICP-OES) assays were performed in a Perkin Elmer Optima 5300 DV instrument. Hg^{2+} quantification was done using a Multi Syringe Flow Inyection (MSFIA) by hydride generation. Elemental Analysis was performed in a LECO CHNS-932 instrument. Melting points are uncorrected.

3-(butylamino)-4-ethoxycyclobut-3-ene-1,2-dione. A solution of n-butylamine (1 mL, 10.1 mmol) in diethyl ether (10 mL) was added dropwise to a stirred solution of diethyl squarate (2 g, 11.8 mmol) in diethyl ether (15 mL). The reaction mixture was stirred overnight at room temperature in an atmosphere of argon. After this period, the solvent was evaporated under vacuum. The yellow oil obtained was washed with pentane (3 x 10 mL) and cold diethyl ether (5 x 10 mL) to finally obtain the product like a white solid. (1.5 g, 75%). Mp=

38ºC. ^{1}H-RMN (DMSO-d_6) δ: 8.79 (br, NH); 8.59 (br, NH); 4.65 (q, 2H); 3.47 (q, 2H); 1.50 (m, 2H); 1.37 (t, 3H); 1.28 (m, 2H); 0.87 (t, 3H) ppm. ^{13}CRMN (DMSO-d_6) δ: 185.42 174.79, 44.25, 33.38, 20.02, 14.34 ppm. FTIR (KBr): 3428, 3212, 2955, 2928, 1816, 1682, 1622, 1543, 1460, 1420, 1362, 1339, 1237, 639 cm^{-1}. HRMS-ES(+) found m/z 417.2002 $[2M+Na]^+$, $C_{20}H_{30}N_2O_6Na$ requires 417.2002.

3-(butylamino)-4-((3,4-dihydroxyphenethyl) amino) cyclobut-3-ene-1,2-dione. To a mixture of sodium carbonate (400 mg; 3.6 mmol) and sodium dithionite (200 mg; 0.59 mmol) was added methanol (10 mL). A solution of 3-hydroxityramine hydrochloride (1.06 g; 5.58 mmol) in methanol (20 mL) was added dropwise to the stirred mixture. Immediately, a solution of 3-(butylamino)-4-ethoxycyclobut-3-ene-1,2-dione (1 g; 5.07 mmol) in methanol (10 mL) was added into the above solution dropwisely too. The pH of the mixture was adjusted at 7 adding 2 drops of NaOH 1M. The reaction mixture was stirred for 2 h at room temperature in an atmosphere of Ar and in absence of light. After this period, the solution was filtered and the resulting solution was stirred overnight in the same conditions. The product is obtained by evaporating the solvent under vacuum. The white solid (**SQ1**) was washed with a mixture 5:1 Et_2O:CH_2Cl_2 (5 x 10 ml). (0.75 g, 49%). Mp= 213ºC. ^{1}H-RMN (DMSO-d_6) δ: 8.57 (br, 2H); 7.80 (br, 2NH); 6.61 (m, 2H); 6.46 (m, 1H); 3.63 (t, 2H); 3.47 (t, 2H); 2.64 (t, 2H); 1.46 (m, 2H); 1.31 (m, 2H); 0.88 (t, 3H) ppm. ^{13}CRMN (DMSO-d_6) δ: 182.67 168.24, 145.44, 144.14, 129.83, 119.94, 116.71, 116.03, 45.53, 43.50, 36.94, 33.30, 19.51, 14.05 ppm. FTIR (KBr): 3170, 2959, 1799, 1649, 1582, 1432, 1357, 1298, 1146, 1112, 951, 815, 757, 614 cm^{-1}. HRMS-ES(+) found m/z 327.1324 $[M+Na]^+$, $C_{16}H_{20}N_2O_4Na$ requires 327.1321.

3-(butylamino)-4-((3,4-dimethoxyphenethyl) amino) cyclobut-3-ene-1,2-dione. A solution of 3-(butylamino)-4-ethoxycyclobut-3-ene-1,2-dione (0.5 g, 2.5 mmol) in methanol (10 mL) was added dropwise to a stirred solution of 3,4-dimethoxyphenethylamine (0.51 mL, 3 mmol) in methanol (20 mL). The reaction mixture was stirred overnight at room temperature in an atmosphere of argon. The product is obtained by evaporating the solvent under vacuum. The white solid **(SQ4)** was washed with cold methanol (5 x 15 mL) and diethyl ether (3 x 10 mL) a white solid. (0.65 g, 80%). Mp= 182ºC. ^{1}H-RMN (DMSO-d_6) δ: 7.34 (br, 2NH); 6.82 (m, 2H); 6.74 (m, 1H); 3.73 (s, 3H); 3.71 (s, 3H); 3.47 (t, 2H); 3.32 (m, 2H); 2.76 (t, 2H); 1.46 (m, 2H); 1.29 (m, 2H); 0.88 (t, 3H) ppm. ^{13}CRMN (DMSO-d_6) δ: 182.54 167.87, 148.75, 147.44, 130.95, 120.73, 112.73, 111.94, 55.52, 44.78, 42.95, 36.66, 33.00, 19.11, 13.62 ppm. FTIR (KBr): 3167, 2957, 1799, 1645, 1575, 1518, 1453, 1384, 1359, 1314, 1144, 1027, 809, 764, 608 cm^{-1}. HRMS-ES(+) found m/z 355.1627 $[M+Na]^+$, $C_{18}H_{24}N_2O_4Na$ requires 355.1634.

Fe_3O_4 nanoparticles functionalized with 3-(butylamino)-4-((3,4-dihydroxyphenethyl) amino) cyclobut-3-ene-1,2-dione. (NP-SQ1). 100 mg of dispersed nanoparticles in hexane were washed three times with methanol and redispersed in methanol. The dispersion was sonicated for 30 min, after which a solution of 3-(butylamino)-4-((3,4-dihydroxy phenethyl) amino) cyclobut-3-ene-1,2-dione (400 mg, 1.31 mmol) in methanol (15 mL) was added and stirred in an atmosphere of argon overnight. After this period, the coated Fe_3O_4 nanoparticles were magnetically separated and washed with a methanol (3 x 10 mL) and redispersed in this solvent. TIR (KBr): 3420, 2924, 1801, 1594, 1543, 1489, 1269, 1117, 588, 420 cm^{-1}.

Fe_3O_4 nanoparticles functionalized with 3-((3,4-dihydroxyphenethyl)amino)-4-((3-(dimethylamino) propyl) amino)cyclobut-3-ene-1,2-dione. (NP-SQ2). 100 mg of dispersed nanoparticles in hexane were washed three times with ethanol and redispersed in this solvent. The dispersion was sonicated for 30 min, after which a solution of 3-((3,4-dihydroxyphenethyl)amino)-4-((3-(dimethylamino) propyl) amino)cyclobut-3-ene-1,2-dione (330 mg, 1 mmol) in ethanol (40 mL) was added and stirred in an atmosphere of argon overnight. After this period, the coated Fe_3O_4 nanoparticles were magnetically separated and washed with ethanol (3 x 10 mL) and redispersed in ethanol. FTIR (KBr): 3443, 1629, 1491, 1275, 583, 440 cm^{-1}.

Fe_3O_4 nanoparticles functionalized with 3-((3,4-dihydroxyphenethyl)amino)-4-((6-((2-((3-(dimethylamino) propyl)amino)-3,4-dioxocyclobut-1-en-1-yl) amino) hexyl) amino) cyclobut-3-ene-1,2-dione. (NP-SQ3). 100 mg of dispersed nanoparticles in hexane were washed three times with ethanol and redispersed in this solvent. The dispersion was sonicated for 30 min, after which a solution of 3-((3,4-dihydroxyphenethyl)amino)-4-((6-((2-((3-(dimethylamino) propyl)amino)-3,4-dioxocyclobut-1-en-1-yl) amino) hexyl) amino) cyclobut-3-ene-1,2-dione (500 mg, 0.95 mmol) in ethanol (5 mL) and DMSO (20 mL) was added and stirred in an atmosphere of argon overnight. After this period, the coated Fe_3O_4 nanoparticles were magnetically separated and washed with a mixture 1:1 of ethanol/DMSO (3 x 10 mL) and redispersed in ethanol. FTIR (KBr): 3420, 3165, 2929, 1801, 1640, 1580, 1431, 1357, 1113, 618 cm^{-1}.

Acknowledgments

This work was supported by Ministerio de Economía y Competitividad ref. CTQ 2011-27152, FEDER funds and Conselleria d´Educació, Cultura i Universitats, Govern de les Illes Balears. Grant FPI09-45692991-H has been co-financed by the European Social Fund. D.Q. thanks the MICINN of Spain for a "Ramón y Cajal" contract.

References

1 M. L. Campbell, D. G. Dixon, R. E. Hecky, J. Toxicol. Environ. Health Part B, 2003, 6, 325-356.

2 J. O. Nriagu, J. M. Pacyna, *Nature*, 1988, **333**, 134-139.

3 N. Rifai, G. Cohen, M. Wolf, L. Cohen, C. Fraser, J. Savory, L. DePalma, *Ther. Drug Monit.,* 1993, **15**, 71-74, and reference therein.

4 J. S. Liu-Fu, *Lead Poisoning, A Century of Discovery and Rediscovery, in Human Lead Exposure*; ed. H. L. Needleman, Lewis Publishing: Boca Raton, FL, 1992.

5 The EPA standard for the maximum allowable amount of Hg^{2+} in drinking water is 2 ppb.

6 D. W. Boening, *Chemosphere,* 2000, **40**, 1335-1351.

7 J. M. Benoit, W. F. Fitzgerald, A. W. Damman, *Environ. Res*., 1998, **78**, 118-133.

8 M. A. R. Meier, U. S. Schubert, *Chem. Commun*. 2005, 4610-4612.

9 R. Haag, *Angew. Chem. Int. Ed*., 2004, **43**, 278-282.

10 M. Liu, K. Kono, J. M. J. Fréchet, *J. Control. Release* 2000, **65**, 121-131.

11 M. S. Diallo, S. Christie, P. Swaminathan, J. H. Johnson Jr, W. A. Goddard III, *Environ. Sci. Technol*. 2005, **39**, 1366-1377.

12 X. Feng, G. E. Fryxell, L.-Q. Wang, A. Y. Kim, J. Liu, K. M. Kemner, *Science*, 1997, **276**, 923-926.

13 U. Wingenfelder, C. Hansen, G. Furrer, R. Schulin, *Environ. Sci. Technol*., 2005, **39**, 4606-4613.

14 Z. Reddad, C. Gerente, Y. Andres, P. Le Cloirec, *Environ. Sci. Technol*., 2002, **36**, 2067-2073.

15 J. Kostal, A. Mulchandani, W. Chen, *Macromolecules* 2001, **34**, 2257-2261.

16 J. Hu, M. C. Lo, G. H. Chen, *Water Sci. Technol*. 2004, **50**, 139-146.

17 J. Hu, G. Chen, M. C. Lo, *Water Res.* 2005, **39**, 4528-4536.

18 Y.-C. Chang, D.-H. Chen, *J. Colloid Interface Sci.,* 2005, **283**, 446-451.

19 A.-F. Ngomsik, A. Bee, M. Draye, G. Cote, V. Cabuil, *C. R. Chimie,* 2005, **8**, 963-970.

20 C. T. Yavuz, J. T. Mayo, W. W. Yu, A. Prakash, J. C. Falkner, S. Yean, L. Cong, H. J. Shipley, A. Kan, M. Tomson, D. Natelson, V. L. Colvin, *Science,* 2006, **314**, 964-967.

21 L.-S. Zhong, J.-S. Hu, H.-P. Liang, A.-M. Cao, W.-G. Sun, L.-J. Wan, *Adv. Mater*., 2006, **18**, 2426-2437.

22 N. Savage, M. S. Diallo, *J. Nanopart. Res.,* 2005, **7**, 331-342.

23 S. M. Ponder, J. G. Darab, T. E. Mallouk, *Environ. Sci. Technol.,* 2000, **34**, 2564-2569.

24 A. M. Donia, A. A. Atia, K. Z. Elwakeel, *J. Hazard. Mat*., 2008, **151**, 372-379.

25 C. L. Warner, W. Chouyyok, K. E. Mackie, D. Neiner, L. V. Saraf, T. C. Droubay, M. G. Warner, R. S. Addleman, *Langmuir,* 2012, **28**, 3931-3937.

26 S. Shin, J. Jang, *Chem. Commun*., 2007, 4230-4232.

27 J.-F. Liu, Z.-S. Zhao, G.-B. Jiang, *Environ. Sci. Technol.,* 2008, **42**, 6949-6954.

28 K. G. Thomas, K. J. Thomas, S. Das, M. V. George, *Chem. Commun*., 1997, 597-598.

29 H. S. Hewage, E. V. Anslyn, *J. Am. Chem. Soc.* 2009, **131**, 13099-13106.

30 H.-C. Lu, W.-T. Whang, B.-M. Cheng, *Chem. Phys. Lett*. 2010, **500**, 267-271.

31 H.-C. Lu, W.-T. Whang, B.-M. Cheng, *J. Mater. Chem*., 2011, **21**, 2568-2576.

32 J. V. Ros-Lis, M. D. Marcos, R. Martínez-Máñez, K. Rurack, J. Soto, *Angew. Chem. Int. Ed*., 2005, **44**, 4405-4407.

33 For characterization of squaramides (SQ1 and SQ4) and functionalized nanoparticles (NP-SQ1, NP-SQ2 and NP-SQ3) see ESI.

34 K. A. López, M. N. Piña, J. Morey, *Synlett*, 2012, **23**, 2830-2834.

35 K. A. López, M. N. Piña, J. Morey, *Sens. Actuators B Chem*., 2013, **181**, 267-273.

36 J. Xie, C. Xu, Z. Xu, Y. Hou, K. L Young, S. X. Wang, N. Pourmond, S. Sun, *Chem. Mater.* 2006, **18**, 5401-5403.

(37) M. Ma, Y. Zhang, W. Yu, H. Y. Shen, H. Q. Zhang, N. Gu, *Colloids Surf. A: Physicochem. Eng. Asp*. 2003, **212**, 219-226.

38 For detailed experimental procedures see ESI.

39 A. M. Serra, J. M. Estela, V. Cerdà, *Talanta*, 2008, **77**, 556-560.

40 G. E. Fryxell, Y. Lin, S. Fiskum, J. C. Birnbaum, H. Wu, K. Kemner, S. Kelly, *Environ. Sci. Technol*., 2005, **39**, 1324-1331.

41 R. R. Avirah, K. Jyothish, D. Ramaiah, *Org. Lett*., 2007, **9**, 121-124.

42 J. W. Steed, J. L. Atwood, *Supramolecular Chemistry*; 2nd ed., John Wiley and Sons Ltd.: Chichester, UK, 2009.

43 L. G. Makarova, A. N. Nesmeyanov, *The Organic compounds of mercury*; North-Holland Publising Co.: Amsterdam, 1967, pp 71-121.

44 H. Satub, K. P. Zeller, H. Leditsche, Houben-Weyl's, *Methoden der Organischen Chemie*; 4th ed., Vol 13, Georg Thieme Verlag, Stuttgart, 1974, Pt. 2b, pp 28-59.

45 B. Gabalov, V. Nikolova, S. Ilieva, *Chem. Eur. J.,* 2013, **19**, 5149-5155.

TOC